Coastal Dynamics 2017
Paper No.044

AN ANALYTICAL SOLUTION FOR LONG WAVES SCATTERING AROUND CIRCULAR ISLANDS WITH FLEXIBLE PROFILE SHAPES

Xiaojing Niu[1]

Abstract

Based on the long wave equation, an analytical solution is obtained for long waves propagating over a circular island mounted on a flat bottom. The profile of the island is idealized as a power function of the radial distance with arbitrary powers. The solution is found by using the separation of variables and the Frobenius method. The newly derived analytical solution is compared with the previous solution. Excellent agreement is found between the two solutions. Then, the effects of island profile on wave distribution are studied. Waves trapped by the island form a complex amplitude distribution pattern in the vicinity of the coastline. Both the average slope and the curvature of the island profile have significant influence to the wave distribution pattern. Resonance may occur, which makes the wave pattern change dramatically even if the geometrical parameters of island profile vary slightly.

Key words: long wave, island, arbitrary slope, analytical solution, Frobenius method

1. Introduction

Tsunami is one of the biggest threats to coastal areas, especially to the island which may directly face the long wave propagating from the deep water. The height of long waves approaching an island can increases several times in the near shore area, and finally run up to a certain elevation into the land, which usually causes great disasters. Unexpected large tsunami billows were observed in the lee of islands in tsunami events such as the tsunami which attacked the Flores Island, Indonesia, on December 12, 1992, and the tsunami which attacked Okushiri Island, Japan, on July 12, 1993. This phenomenon greatly interested researchers in coastal engineering field, and has been proved as a consequence of refractive focusing or resonance of virtually trapped waves.

Many studies have been carried out on the scattering of waves around a circular island. Lautenbacher (1970) derived an integral equation to solve this problem. Smith and Sprinks (1975) studied this problem numerically by using the mild-slope equation. Liu et al (1995) studied the solitary waves climbing up a circular island numerically based on the two-dimensional shallow-water wave equations, and compared with the large-scale laboratory experiments of tsunami runup on a circular island carried out by Briggs et al. (1995). There are also several analytical studies on long waves scattering around an island, which may be more useful to understand the mechanics of the phenomena. As early as 1950, Homma (1950) studied long waves around a cylinder mounted on a parabolic shoal. Zhang and Zhu (1994) obtained an analytical solution of the long wave equation for long waves around a conical island. Zhu and Zhang (1996) obtained a solution for a cylinder mounted on a conical shoal. There are also some analytical studies focused on other axis-symmetric topographies, such as a submerged truncated paraboloidal shoal (Lin and Liu, 2007), a circular hump (Zhu and Harun, 2009), a circular pit (Suh et al., 2005; Jung and Suh, 2008). However, most solutions are limited to cases in which topography is expressed as a certain integral power of the radial distance. Only a few solutions were obtained for the topography described by a power function of the radial distance with arbitrary powers. Yu and Zhang (2003) obtained a solution for a cylinder mounted on a circular shoal with relatively general geometry, in which the profile of the shoal is a power function of arbitrary power. Niu and Yu (2011) derived a solution for a circular submerged hump described by a power function of arbitrary power plus a constant.

[1] Department of Hydraulic Engineering, Tsinghua University, Beijing, China. nxj@tsinghua.edu.cn

In this study, we focus on the problem that long waves scattering around a circular island, in which the water depth around the island varies in proportion to an arbitrary power of the radial distance. The idealized physical problem is shown in Figure 1. The same problem has been studied by Jung et al. (2010). In their study, Taylor series expansion is used to make the governing equation solvable. A new method will be introduced to find the analytical solution in this study, which is expressed in Section 2. Then the solution is compared with that of Jung et al. (2010), and the effect of island profile on wave propagation is discussed.

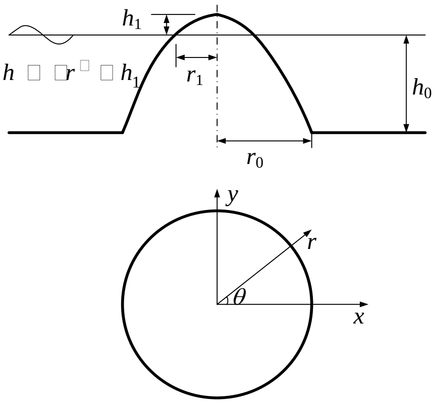

Figure 1. Sketch of the physical problem

2. General solution

The long wave equation is applied to describe linear long waves passing over an axial symmetrical bathymetry without energy dissipation, which can be written in polar coordinates (r, q) as following.

$$r^2 \frac{\partial^2 \eta}{\partial r^2} + r\left(1 + \frac{r}{h}\frac{\partial h}{\partial r}\right)\frac{\partial \eta}{\partial r} + \frac{\partial^2 \eta}{\partial \theta^2} + \frac{\sigma^2 r^2}{gh}\eta = 0 \tag{1}$$

where η is the complex-numbered water surface elevation with its modulus representing the conventional wave amplitude and its argument representing the relative phase, h is the local water depth which is a function of the horizontal coordinates, σ is the wave angular frequency, g is the gravity acceleration.

By separation of variables, the water surface elevation can thus be expressed by

$$\eta(r,\theta) = \sum_{n=0}^{\infty} R_n(r)(D_n \cos n\theta + E_n \sin n\theta) \tag{2}$$

where D_n and E_n are constants, and $R_n(r)$ is a function of r satisfying the following ordinary differential equation.

$$r^2 \frac{d^2 R_n}{dr^2} + r\left(1 + \frac{r}{h}\frac{dh}{dr}\right)\frac{dR_n}{dr} + \left(\frac{\sigma^2 r^2}{gh} - n^2\right)R_n = 0 \tag{3}$$

Assume that the water depth in the problem of interest is expressed by

$$h(r) = \beta r^{\alpha} - h_1 \tag{4}$$

where r is the distance away from the crest of the island, h_1 is a positive constant representing the height of the island above still water surface, α and β are parameters which jointly determine the shape of the island. Substituting Eq. (4) into Eq. (3) results in

$$(\beta r^{\alpha}-h_1)r^2\frac{d^2R_n}{dr^2}+r\left[(\alpha+1)\beta r^{\alpha}-h_1\right]\frac{dR_n}{dr}+\left[\frac{\sigma^2r^2}{g}-n^2(\beta r^{\alpha}-h_1)\right]R_n=0 \tag{5}$$

In case of $h_1=0$, it is noted that the problem degenerates to that solved by Yu and Zhang (2003). Eq.(5) then can be transformed into Bessel's equation of real orders. However, when $h_1\neq 0$, it is hard to transform Eq.(5) into a known special equation. Thus we turn to finding a solution by using the Frobenius type series.

Before applying the Frobenius method to Eq. (5), a mapping should be introduced into Eq. (5), in order to make sure that the physical domain of interest is located within a convergent region of the series solution. And the Frobenius method is useful in finding solution of the differential equation whose coefficients are polynomials. In case that α is not an integer, the coefficients of all the terms in Eq. (5), $(\beta r^{\alpha}-h_1)r^2$, $r\left[(\alpha+1)\beta r^{\alpha}-h_1\right]$, $\sigma^2r^2/g-n^2(\beta r^{\alpha}-h_1)$, cannot be expanded in polynomial form with finite terms.

In the study of Jung et al. (2010), they used the Taylor series expansion to deal with the coefficient which is not in polynomial form and transformed it into an infinite series. To avoid that coefficients being infinite series, a new transform is introduced in the present study. It is no doubt that the arbitrary real constant α can be expressed or approximately expressed as a fraction, written as $\alpha=p/q$. In which p, q are positive integers. Then a mapping is introduced to Eq. (5)

$$t=1-\left(\frac{r_1}{r}\right)^{\frac{1}{q}} \tag{6}$$

Then we have

$$\begin{aligned}&\left[1-(1-t)^p\right](1-t)^2\frac{d^2R_n}{dt^2}+(1-t)\left[p-1+(1-t)^p\right]\frac{dR_n}{dt}\\&+\left[q^2(1-t)^{p-2q}v^2-n^2q^2\left[1-(1-t)^p\right]\right]R_n=0\end{aligned} \tag{7}$$

where

$$v^2=\frac{\sigma^2}{gh_1}r_1^2 \tag{8}$$

It is known that $(1-t)^p$ can be expanded in polynomial form as

$$(1-t)^p=\sum_{k=0}^{p}C_p^k(-1)^kt^k \tag{9}$$

In which, C_p^k is the combinational formula. Here, it is defined as

$$C_p^k=\begin{cases}\dfrac{p!}{(p-k)!k!}, & 0\le k\le p\\ 0, & other\end{cases} \tag{10}$$

It is clear that the coefficient of each term in Eq. (7) can be expanded in polynomial form, when $p-2q\ge 0$, i.e., $\alpha\ge 2$. Otherwise Eq. (7) multiplied with $(1-t)^{2q-p}$ will be solved, when $p-2q<0$, i.e., $\alpha<2$. And the Based on Frobenius' theory, the following series solution is assumed.

$$R_n = \sum_{m=0}^{\infty} a_m t^{m+c} \tag{11}$$

In which, a_m and c are coefficients to be determined. It can be proved that the series solution converges for $|t|<1$, and the convergent region can cover the physical domain of interest in this study. After submitting Eq.(11) into Eq.(7) and collecting terms with the same order of t, the solution of c is obtained by equating the coefficient of the lowest order of t to zero.

$$c = 0 \tag{12}$$

It is a double repeated root. One particular solution of R_n can always be obtained as

$$R_n = \sum_{m=0}^{\infty} a_m t^{m} \tag{13}$$

Another independent particular solution contains logarithmic terms, which is singular at $t=0$. However, in present study the water surface elevation is finite at the coastline ($t=0$), so this particular solution does not appear in the final solution. Only the solution in Eq. (13) is formulated, the coefficient in Eq.(13) is obtained as

$$a_1 = -\frac{q^2 v^2}{p} \tag{14}$$

In case of $p-2q>0$, i.e., $\alpha \geq 2$,

$$m \geq 2,\ a_m = -\frac{A_{0,m-1}a_{m-1} + \sum_{k=1}^{\min(m-1,p)} A_{k,m-k-1}a_{m-k-1}}{pm^2} \tag{15}$$

where

$$A_{0,m} = -(0.5p^2+1.5p)m^2 + (0.5p^2-0.5p)m + q^2v^2 \tag{16}$$

$$\begin{aligned} A_{k,m} = (-1)^k \Big[& -(C_p^{k+2}+2C_p^{k+1}+C_p^k)m^2 + (C_p^{k+2}+C_p^{k+1})m \\ & + n^2q^2C_p^k + q^2v^2C_{p-2q}^k \Big] \end{aligned} \tag{17}$$

In case of $p-2q<0$, i.e., $\alpha<2$,

$$m \geq 2, a_m = -\frac{A_{0,m-1}a_{m-1} + \sum_{k=1}^{\min(m-1,2q)} A_{k,m-k-1}a_{m-k-1}}{pm^2} \tag{18}$$

where

$$A_{0,m} = (C_{2+2q-p}^2 - C_{2+2q}^2)(m^2-m) - (2+2q-p)pm + q^2v^2 \tag{19}$$

$$\begin{aligned} A_{k,m} = (-1)^k \Big[& (C_{2+2q-p}^{k+2} - C_{2+2q}^{k+2})(m^2-m) \\ & - \left[(p-1)C_{1+2q-p}^{k+1} + C_{1+2q}^{k+1}\right]m - n^2q^2(C_{2q-p}^k - C_{2q}^k) \Big] \end{aligned} \tag{20}$$

By the original variable r, the solution can be written as

$$R_n = \sum_{m=0}^{\infty} a_m \left[1 - \left(\frac{r_1}{r} \right)^{\frac{1}{q}} \right]^m \tag{21}$$

3. Solution for a circular island on a flat bottom

The physical problem of interest in this section is long wave scattering around a circular island on an otherwise flat bottom, as shown in Figure 1. The water depth over the entire domain is described by

$$h(r) = \begin{cases} \beta r^{\alpha} - h_1, & r_1 \le r \le r_0 \\ h_0, & r_0 < r \end{cases} \tag{22}$$

in which, α and β are parameters which jointly determine the shape of the island. h_1 is the height of the island above still water surface, r_1 is the radius of island above still water surface, h_0 is the water depth over the flat bottom, r_0 is the radius distance from the center to the toe of the island in the horizontal plane. The domain concerned is divided into two regions: the outer region with constant water depth ($r_0 < r$) and the inner region with variable water depth ($r_1 \le r \le r_0$).

We assume that the incident wave is a long-crested sinusoidal wave propagating in the positive x direction. The water surface elevation in the outer region is given by MacCamy and Fuchs (1954), which is expressed by

$$\eta_1 = A_I \sum_{n=0}^{\infty} i^n \varepsilon_n J_n(k_0 r) \cos n\theta + \sum_{n=0}^{\infty} B_n H_{1n}(k_0 r) \cos n\theta \tag{23}$$

In which, the first term corresponds to the incident wave and the second term corresponds to the scattered wave. A_I is the incident wave amplitude, $i = \sqrt{-1}$, k_0 is the wavenumber over the flat bottom in the outer region ($k_0 = \sigma / \sqrt{g h_0}$ for long waves), B_n are complex-valued constants to be determined, J_n is the Bessel function of the first kind and the n-th order; H_{1n} is the Hankel function of the first kind and the n-th order; and ε_n is the Jacobi symbol defined by

$$\varepsilon_n = \begin{cases} 1, & n = 0 \\ 2, & n \ge 1 \end{cases} \tag{24}$$

The general solution of the water surface elevation in the inner region is available from the previous section. Considering that the problem under consideration is symmetrical with respect to x-axis, we have

$$\eta_2 = \sum_{n=0}^{\infty} D_n R_n(r) \cos n\theta \tag{25}$$

On the other hand, the patching conditions at the common boundary of the two regions, i.e., at $r = r_0$, require

$$\eta_1 = \eta_2 \quad (r = r_0) \tag{26}$$

$$\frac{\partial \eta_1}{\partial r} = \frac{\partial \eta_2}{\partial r} \quad (r = r_0) \tag{27}$$

Result in

$$B_n = -\frac{A_1 i^n \varepsilon_n \left[R_n(r_0) k_0 J_n'(k_0 r_0) - R_n'(r_0) J_n(k_0 r_0) \right]}{R_n(r_0) k_0 H_{1n}'(k_0 r_0) - R_n'(r_0) H_{1n}(k_0 r_0)} \tag{28}$$

$$D_n = \frac{2 A_1 i^{n+1} \varepsilon_n}{\pi r_0 \left[R_n(r_0) k_0 H_{1n}'(k_0 r_0) - R_n'(r_0) H_{1n}(k_0 r_0) \right]} \tag{29}$$

The boundary condition at the coastline request the normal flux at the coastal line is zero (Mei, 1989), which is written as

$$\lim_{r \to r_1} h \frac{\partial \eta_2}{\partial r} = 0 \tag{30}$$

Obviously, Eq. (30) is automatically satisfied in this solution.

So far, we have derived a novel solution for long waves scattering around a circular island. In contrast to the study of Jung et al. (2010), the present solution does not rely on the Taylor series expansion.

4. Comparison with previous solution

4.1. *Validation with the previous study*

In this section, the present solution is compared with that obtained by Jung et al. (2010). In order to validate the present solution, we compared the present solution to that of Jung et al. (2010) for long waves passing over an island with different parameters α . The parameters of the islands used were $r_1 = 10\text{km}$, $h_0 = 4\text{km}$, $r_0 = 30\text{km}, 90\text{km}$, and $\alpha = 2/3,\ 1,\ 2$. The incident wave periods is T=720s. Figure 2 shows the variation of relative wave amplitudes along the coastline, in which solid lines represent results of the present solution and dots represent results by Jung et al. (2010). It can be seen that the calculated wave runup along the coastline by the present solution agrees very well with that of Jung et al. (2010).

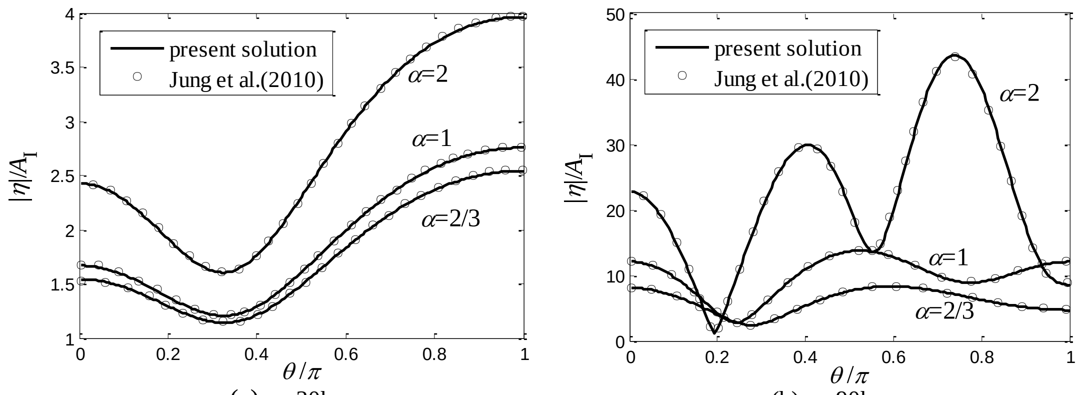

Figure 2. Compare the present solution with that of Jung et al. (2010)

4.2. *Convergence of the series*

The main difference between the present solution and that of Jung et al.(2010) is the solution in the inner region with variable water depth. The solution of R_n is an infinite series. In practice, the series should be truncated as a finite series with M terms within a certain tolerance.

$$R_n \approx R_n{}^M \equiv \sum_{m=0}^{M} a_m \left[1 - \left(r_1/r \right)^{\frac{1}{q}} \right]^m \tag{31}$$

From the expression of R_n, we can easily conclude that the series is harder to converge with large r in case other parameters keep constants. In case that T=720s, r_1=10km, h_0=4km, α =2, r_0=3r_1, we calculated the series of R_n by trial and error with a truncation error $\left|(R_n^{\ M} - R_n^{\ M-1})/R_n^{\ M}\right| < 10^{-6}$. Obviously the larger r/r_1, the more terms, or the larger M, are needed to get the converging value of R_n. It is also found that the larger n corresponds with the larger M, as shown in Figure 3(a). Here, r=r_0 is used for getting the maximum M. Comparing the present solution with that of Jung et al. (2010), it can be clearly seen that the present solution is easier to converge within the certain tolerated error in some cases.

We also check the influence of the parameter α on R_n, while retain the other parameters including r=r_0 and n=0. The power α is chosen to be 1/4, 1/3, 1/2, 2/3, 3/4, 1, 3/2, 2, 5/2, 3. The number of terms remained M is obtained by trial and error, shown in Figure 3(b). Circles represent the results of present solution, and triangles represent that of Jung et al. (2010). The number M shows a rising trend as the parameter α increases by using the solution of Jung et al. (2010). In case that α equals 1/4, 1/3, 1/2, 1, the convergence of the present solution is same with that of Jung et al. (2010). However, in most cases, especially α larger than 1, the present solution converges faster than the solution of Jung et al. (2010).

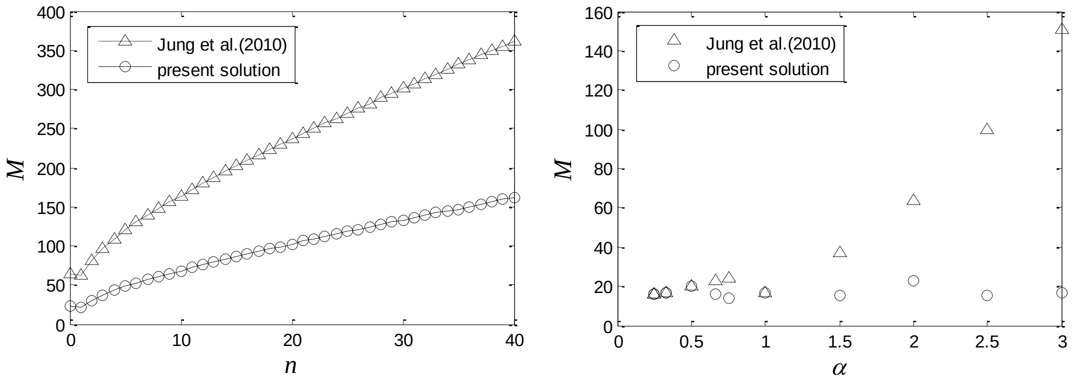

(a) M vs. n (b) M vs. α

Figure 3. The influence of n and α on the convergence of R_n

5. Results and discussions

In this section, the effects of the island profile on wave refraction and diffraction are studied by using the derived analytical solution. Considering a circular island with known radius r_1 and the water depth in the surrounding flat area h_0 is fixed, there are two geometric parameters that control the underwater profile of the island. One is the radius of underwater part r_0, the other is the parameter α representing the curvature of the profile. The change of r_0 is equivalent to changing the average slope of underwater profile.

5.1. *The distribution pattern of wave amplitude*

Figure 4 gives a global view of the relative wave amplitude $|\eta|/A_I$ corresponding to r_0=3r_1, 6r_1, 9r_1, 12r_1, while the other parameters are fixed. Here, r_1=10km, h_0=4km, $\alpha = 1$ and the period of incident long wave T=720s. In Figure 4, the solid circle shows the coastline of the island and the broken circle shows the toe of the island. All the results show that the wave amplitude is large in the vicinity of the coastline. It suggests a concentration of wave energy near the coastline due to refraction and diffraction. In some cases, wave amplitude is much amplified, because incident waves in a large area have been trapped near the coastline. More incident waves possibly reach the vicinity of the coastline in the case of a mild slope. So the wave amplitude near the coastline becomes higher and its distribution turns more complex as r_0 increases.

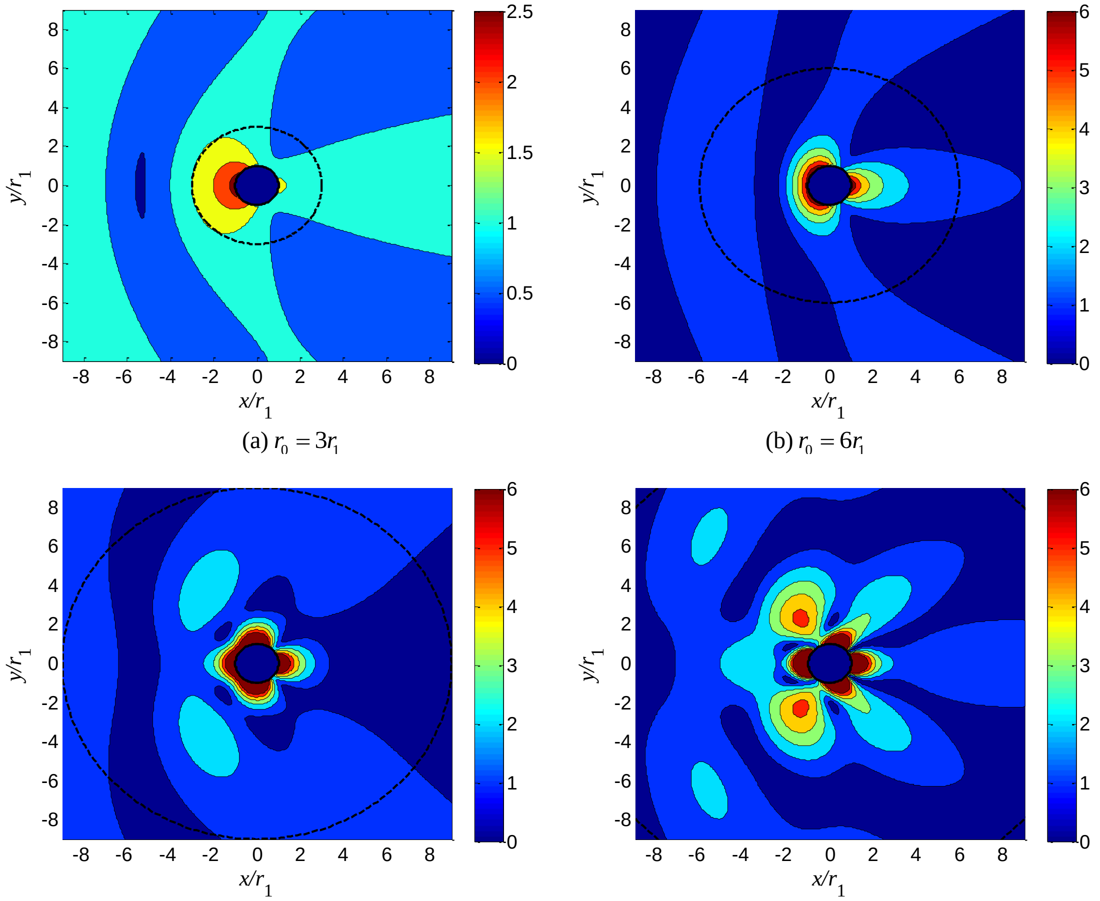

(a) $r_0 = 3r_1$ (b) $r_0 = 6r_1$

(c) $r_0 = 9r_1$ (d) $r_0 = 12r_1$

Figure 4. Contour of relative wave amplitude corresponding to different r_0

Figure 5 shows the profile of the island corresponding to $\alpha = 1/3,\ 2/3, 1.3, 1.6, 2, 2.5$ with fixed r_1, r_0 and h_0. The profile is convex at $\alpha > 1$ and is concave at $\alpha < 1$. The larger α corresponds with a steeper slope at the toe and milder slope near the water surface. Figure 6 shows the contour of relative wave amplitudes around the island with different α, while the other parameters are fixed as r_0=9r_1, r_1=10 km, h_0=4 km and the wave period is T=720s. It is noticeable that not only the average slope has great influence on wave amplitude distribution around the island, but also the curvature parameter α. The larger α results in more energy concentration near the coastline and a more complex wave distribution pattern. But the maximum wave amplitude and the area of high wave do not grow monotonously as the parameter α increases. It can be clearly seen that the area of the relative wave amplitude greater than 6 is much larger in the case of $\alpha = 1.3$ than in the cases of $\alpha = 1$ and $\alpha = 1.6$, as shown in Figure 6(c), Figure 4(c) and Figure 6(d).

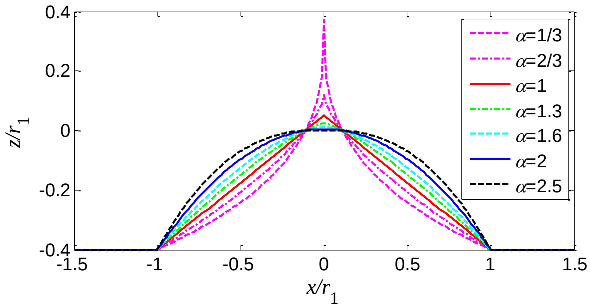

Figure 5. Island profile corresponding to different values of α

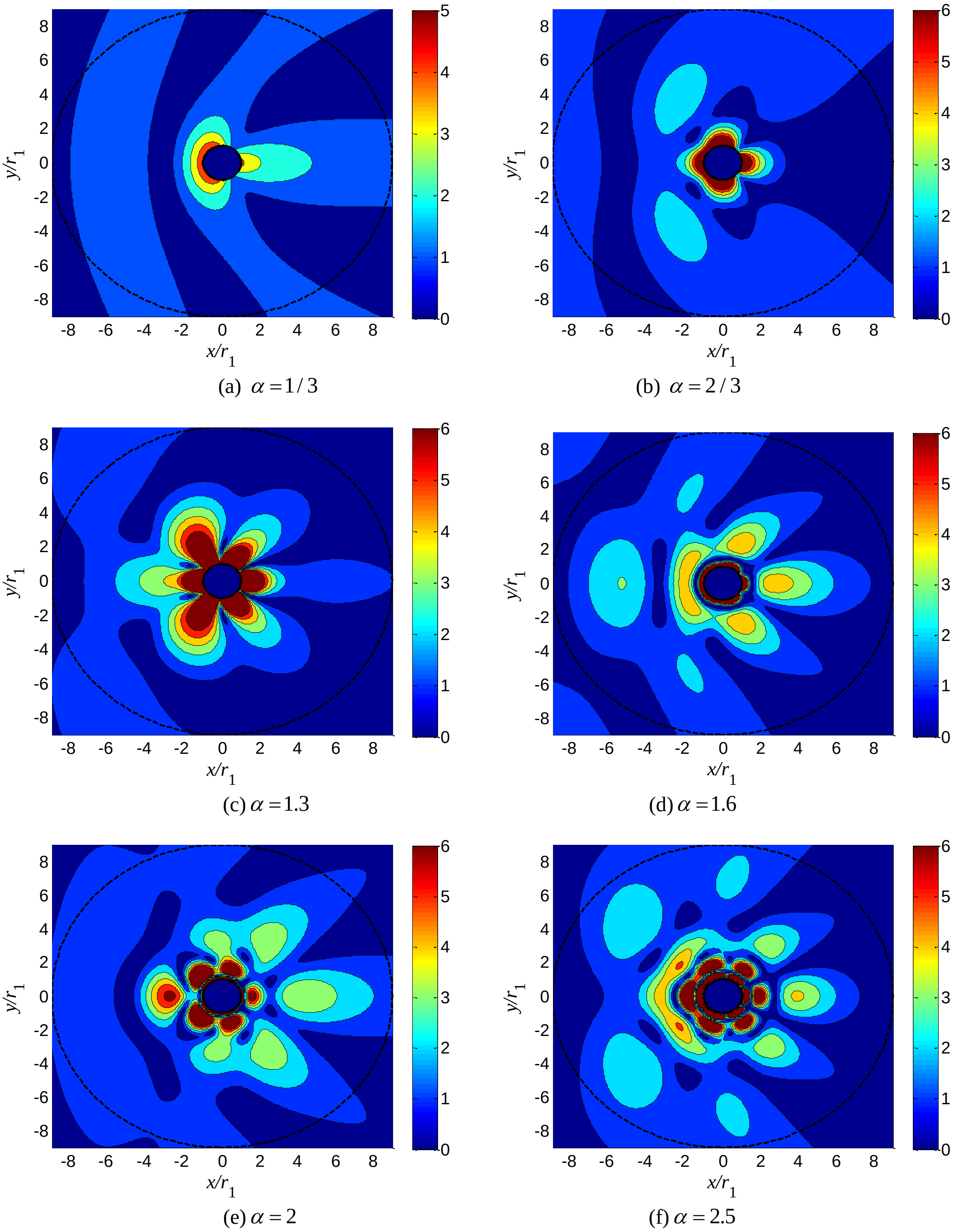

(a) $\alpha = 1/3$ (b) $\alpha = 2/3$

(c) $\alpha = 1.3$ (d) $\alpha = 1.6$

(e) $\alpha = 2$ (f) $\alpha = 2.5$

Figure 6. Contour of relative wave amplitude corresponding to different values of α

5.2. *The frequency variation of the amplitude factors*

In order to get better understanding of the complex distribution of wave amplitude, the modal responses of waves to the island is analyzed. Waves in the vicinity of the island are expressed by Eq. (25) as a series of partial waves with an angular dependence of $\cos n\theta$. Here, the solution corresponding to $\cos n\theta$ is called as the *n*-th mode of wave. As R_n=1 when r=r_1, the coefficient D_n is the amplitude factor of each mode of wave at the coastline, which is a good indicator to show the modal responses of waves to the island.

The value of D_n is determined by three independent parameters, the dimensionless wave frequency, the average slope and the curvature of the island. Figure 7 and Figure 8 show the absolute value of D_n for primary modes as a function of the incident wave frequency in the cases of different average slopes or different curvature parameters. In Figure 7, the curvature parameter α is fixed to be 1 in all the cases and varying r_0 is to change the average slope of island profile. In Figure 8, α is changed while the average slope is fixed.

Generally, the value of D_n increases at low frequency and tends to a constant at high frequency. For waves of very low frequency, D_n tends to1 in the lowest mode and decreases quickly as the mode n increase. The number of dominant modes increases as the incident wave frequency increases for a certain island. So the wave scattered by the island shows more complex distribution pattern as wave frequency increase, because the higher mode forms a more complex wave pattern.

The variation of D_n between the low and high frequency is not monotonous. Resonance phenomenon can be found for larger n. It means that much higher waves near the coastline will be formed if the wave frequency is near the resonant peaks. In the case of the island with $\alpha = 1.3$, the resonant peak of the third mode is about $r_1\sigma\left(h_0 g\right)^{-1/2} \approx 0.44$, corresponding to the wave period $T \approx 720\mathrm{s}$. That is why especially large waves occur in the case of $\alpha = 1.3$, as shown in Figure 6(c).

The resonant peaks shift to the high frequency side as n increases. Increasing n leads to much larger and sharper resonant peaks. A larger peak value implies large wave amplitude around the coastline when the corresponding mode has been excited. While a sharper peak implies that the corresponding mode is more difficult to be excited in natural marine environment.

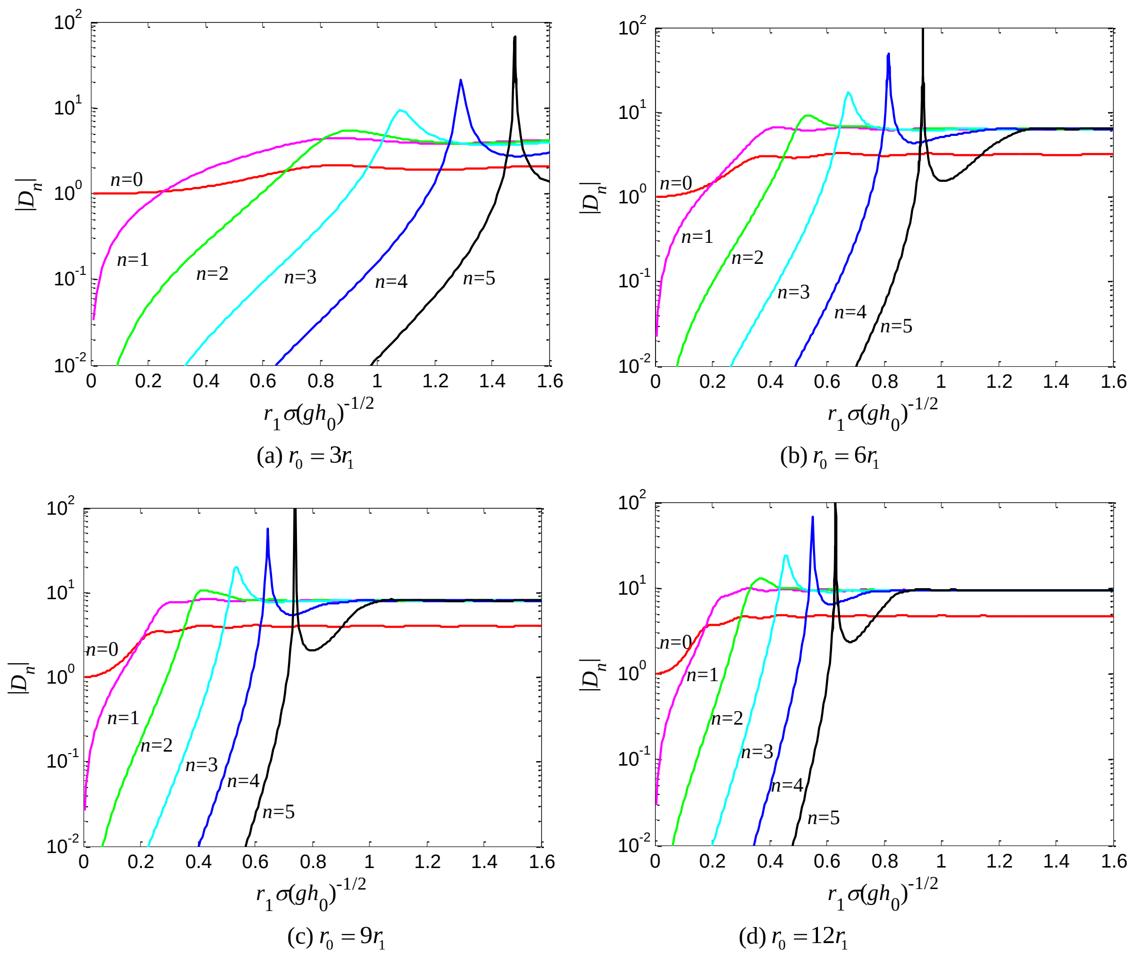

Figure 7. Frequency dependence of the amplitude factors D_n corresponding to different r_0

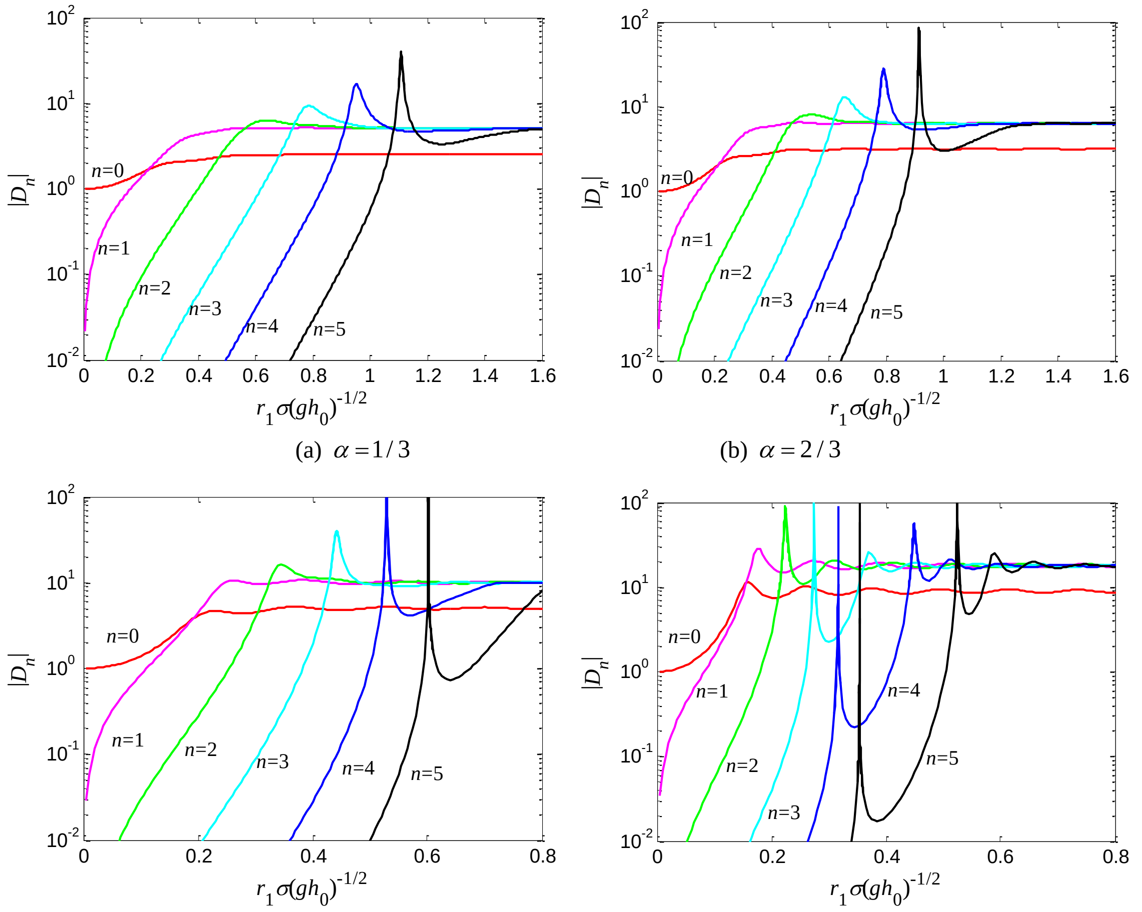

(a) $\alpha = 1/3$ (b) $\alpha = 2/3$

(c) $\alpha = 1.3$ (d) $\alpha = 2$

Figure 8. Frequency dependence of the amplitude factors D_n corresponding to different α

The shape of island profile has significant impact on the curve of D_n. The increase of r_0 causes the resonant peaks of all modes move toward lower frequency. It suggests that longer wave can be trapped by the island with larger r_0 or milder average slope. There is only one significant resonant peak in the first six modes when α is small, as shown in Figure 8(a), 8(b) and 8(c). But more resonant peaks occur when α =2, as shown in Figure 8(d). The resonant peaks also move toward lower frequency as α increases. This implies more complex wave distribution pattern corresponding to larger α .

6. Conclusion

In this study, we derived a new analytical solution for long waves scattering around an island. The island is idealized to be axial symmetrical and its radial profile can be described by a power function with arbitrary powers. The water depth around the island is expressed as $h(r) = \beta r^{\alpha} - h_1$, in which α , β , h_1 are three independent parameters. The linear long waves passing over an axial symmetrical bathymetry without energy dissipation is described by a long wave equation written in polar coordinates. And the equation is then solved by separation of variables and the Frobenius method.

The Frobenius method is useful in finding solution of the differential equation whose coefficients are polynomials. In this case, if the profile parameter α is not an integer, the coefficients of the derived differential equation cannot be directly written in polynomials, it will rise a great difficulty to solve the equation. In the study of Jung et al. (2010), they used the Taylor series expansion to deal with the coefficient which is not in polynomial form and transformed it into an infinite series. To avoid that coefficients being infinite series, a new transform is introduced in the present study. First, the arbitrary real constant α is expressed or approximately expressed as a fraction, written as $\alpha=p/q$. Then a mapping is introduced, which can successfully make the equation solvable.

The newly derived solution was compared with the previous solution obtained by Jung et al. (2010). The cores of the two solutions are totally of different expression, because different derivation method was used to get the general solution in the inner region with variable water depth. By applying the two analytical solutions to the same cases, it can be seen that the present solution agrees well with that of Jung et al. (2010). By comparing the convergence of the series solution, it shows that the present solution is superior to that of Jung et al. (2010) in most cases.

Based on the derived solution, the effects of the island profile on wave distribution are discussed. The analytical results reveal that not only the average slope but also the curvature parameter has great influence on wave amplitude distribution around the island. Generally, the larger curvature parameter and the smaller average slope result in more complex wave distribution pattern and higher wave amplitude near the coastline of island. But wave amplitude is not monotonously varying as gradually changing the geometrical parameter of island profile. Resonance phenomenon makes the variation of wave pattern more complex. The resonant frequency is found increasing as the average slope increase and decreasing as the curvature parameter increase.

Acknowledgements

The author would like to acknowledge the support by the National Natural Science Foundation of China under the grant No. 51479101 and Tsinghua University Initiative Scientific Research Program.

References

Homma, S., 1950. On the behaviour of seismic sea waves around circular island. *Geophys. Mag.*, 21:199-208.

Jung, T.-H. and Suh, K.-D., 2008. An analytical solution to the extended mild-slope equation for long waves propagating over an axi-symmetric pit. *Wave Motion*, 45: 835-845.

Jung,T.-H., Lee, C., and Cho, Y.-S., 2010. Analytical solution for long waves over a circular island. *Coastal Engineering*, 57 :440-446.

Lautenbacher, C. C., 1970. Gravity wave refraction by islands. *Journal of Fluid Mechanics*, 41: 455- 672.

Lin, P. and Liu, H., 2007. Scattering and trapping of wave energy by a submerged truncated paraboloidal shoal. *Journal of Waterway, Port, Coastal, and Ocean Engineering*, 133(2): 94-103.

Longuet-Higgins, M.S., 1967. On the trapping of wave energy round islands. *Journal of Fluid Mechanics*, 29: 781-821.

MacCamy, R. C. and Fuchs, R. A., 1954. Wave forces on piles: a diffraction theory. Technical Memorandum No. 69, Beach Erosion Board, U. S. Army Corps of Engineers.

Mei, C.C., 1989. *The Applied Dynamics of Ocean Surface Waves*, World Scientific.

Niu, X. and Yu, X., 2011. Analytic solution of long wave propagation over a submerged hump. *Coastal Engineering*, 58: 143-150.

Smith, R. and Sprinks, T., 1975. Scattering of surface waves by a conical island. *Journal of Fluid Mechanics*, 72: 373-384.

Suh, K.-D., Jung, T.-H., and Haller, M. C., 2005. Long waves propagating over a circular bowl pit. *Wave Motion*, 42: 143-154.

Yu, X. and Zhang, B., 2003. An extended analytic solution for combined refraction and diffraction of long waves over circular shoals. *Ocean Engineering.*, 30: 1253-1267.

Zhang, Y., and Zhu, S., 1994. New solutions for the propagation of long water waves over variable depth. *Journal of Fluid Mechanics*, 278: 391-406.

Zhu, S.-P. and Harun, F. N., 2009. An analytical solution for long wave refraction over a circular hump. *Journal of Applied Mathematics and Computing*, 30: 315-333.

Zhu, S.-P. and Zhang, Y., 1996. Scattering of long waves around a circular island mounted on a conical shoal. *Wave Motion*, 23: 353-362.